N A T U R A L R E S O U R C E S

TSUNAMI HAZARD MAPS OF THE ANACORTES–BELLINGHAM AREA, WASHINGTON—MODEL RESULTS FROM A ~2,500-YEAR CASCADIA SUBDUCTION ZONE EARTHQUAKE SCENARIO

by Daniel W. Eungard, Corina Forson, Timothy J. Walsh, Edison Gica, and Diego Arcas

WASHINGTON
GEOLOGICAL SURVEY
Map Series 2018-02
June 2018

[Superseded by Map Series 2021-01]

INTERNALLY REVIEWED

WASHINGTON STATE DEPARTMENT OF
NATURAL RESOURCES
WASHINGTON GEOLOGICAL SURVEY

THIS PUBLICATION HAS BEEN SUPERSEDED BY MAP SERIES 2021-01

TSUNAMI HAZARD MAPS OF THE ANACORTES–BELLINGHAM AREA, WASHINGTON—MODEL RESULTS FROM A ~2,500-YEAR CASCADIA SUBDUCTION ZONE EARTHQUAKE SCENARIO

by Daniel W. Eungard, Corina Forson, Timothy J. Walsh,
Edison Gica, and Diego Arcas

WASHINGTON
GEOLOGICAL SURVEY
Map Series 2018-02
June 2018

[Superseded by Map Series 2021-01]

This publication has been subject to an iterative technical review process by at least one Survey geologist who is not an author. This publication has also been subject to an iterative review process with Survey editors and cartographers and has been formatted by Survey staff.

WASHINGTON STATE DEPARTMENT OF
NATURAL RESOURCES
WASHINGTON GEOLOGICAL SURVEY

INDEMNIFICATION

This item was funded by a National Tsunami Hazard Mitigation Program grant (award no. NA17NWS4670017) to the Washington Geological Survey from the Department of Commerce/National Oceanic and Atmospheric Administration. This does not constitute an endorsement by NOAA. Information about NTHMP is available at http://nws.weather.gov/nthmp/.

Washington State Department of Natural Resources
Washington Geological Survey

Mailing Address:
MS 47007
Olympia, WA 98504-7007

Street Address:
Natural Resources Bldg, Rm 148
1111 Washington St SE
Olympia, WA 98501

Phone: 360-902-1450
Fax: 360-902-1785
Email: geology@dnr.wa.gov
Website: http://www.dnr.wa.gov/geology

Publications and Maps:
www.dnr.wa.gov/programs-and-services/geology/publications-and-data/publications-and-maps

Washington Geology Library Searchable Catalog:
www.dnr.wa.gov/programs-and-services/geology/washington-geology-library

Suggested Citation: Eungard, D. W.; Forson, Corina; Walsh, T. J.; Gica, Edison; Arcas, Diego, 2018, Tsunami hazard maps of the Anacortes–Bellingham area, Washington—Model results from a ~2,500-year Cascadia subduction zone earthquake scenario: Washington Geological Survey Map Series 2018-02, superseded by Map Series 2021-01, 6 sheets, scale 1:30,000, 10 p. text. [http://www.dnr.wa.gov/publications/ger_ms2018-02_tsunami_hazard_anacortes_bellingham.zip]

State of Washington
3151
Licensed Geologist
Daniel W Eungard

June 2018

Contents

Tsunami Hazard Maps of the Anacortes–Bellingham Area, Washington—Model Results from a ~2,500-year Cascadia Subduction Zone Earthquake Scenario

by Daniel W. Eungard[1], Corina Forson[1], Timothy J. Walsh[1], Edison Gica[2], and Diego Arcas[2]

[1] Washington Geological Survey
MS 47007
Olympia, WA 98504-7007

[2] National Oceanic and Atmospheric Administration
Pacific Marine Environmental Laboratory
7600 Sand Point Way NE
Seattle, WA 98115-6349

ABSTRACT

New finite-difference tsunami inundation modeling in the areas surrounding Anacortes and Bellingham uses a simulated magnitude 9 earthquake event with a maximum slip of ~89 ft (27 m), inferred to be a ~2,500-year event, called the L1 scenario. This new modeling closely approximates the design requirements in the building code standard for critical facilities, and is more conservative (greater inundation) than previous tsunami modeling. Modeling results indicate that the first tsunami wave trough will reach the study area approximately one and a half hours following the earthquake. Inundation depths may reach as much as 18 ft (5.5 m). Current velocities from the tsunami waves locally exceed 20 knots, presenting a significant navigational hazard to the maritime community. Tsunami wave inundation is expected to continue over 8 hours and remain hazardous to maritime operations for more than 24 hours. This study is limited in that modeling does not account for changes in tide stage, liquefaction, or minor topographic changes that would locally modify the effects of tsunami waves. Due to these limitations, this modeling should not be used for site-specific tsunami inundation assessment or for determining effects on the built environment. However, this model is a useful tool for evacuation and recovery planning.

INTRODUCTION

In 1995, Congress directed the National Oceanic and Atmospheric Administration (NOAA) to develop a plan to protect the west coast from tsunamis generated by the nearby Cascadia subduction zone (CSZ). A panel of representatives from NOAA, the Federal Emergency Management Agency (FEMA), the U.S. Geological Survey (USGS), and the five Pacific coast states wrote and submitted the plan to Congress, which created the National Tsunami Hazard Mitigation Program (NTHMP) in October of 1996. The NTHMP is designed to reduce the impact of tsunamis through warning guidance, hazard assessment, education, and mitigation.

A key component of the hazard assessment for tsunamis is delineation of areas subject to tsunami inundation. Because local tsunami waves may reach nearby coastal communities within one or two hours after the earthquake, there will be limited time to issue formal warnings and direct evacuees. To expedite the evacuation process, evacuation areas and routes will need to be planned well in advance.

Map Sheets 1 through 6 depict modeled tsunami inundation and current velocity for the Anacortes and Bellingham area from a CSZ earthquake (Fig. 1); they are part of a series of tsunami inundation maps produced by the Washington Geological Survey, in cooperation with the Washington Emergency Management Division, as a contribution to the NTHMP (Table 1). These maps are produced using computer models of earthquake-generated tsunamis from the CSZ developed by the Pacific Marine Environmental Laboratory (PMEL)

Previous inundation modeling for this area (Walsh and others, 2004, 2005) was for an event on the CSZ using the 1A and 1A with asperity scenarios (Myers and others, 1999; Priest and others, 1997). The 1A scenario was generated prior to the development of any federal or state building code standards for tsunami hazards. For several years, it was the only source of tsunami hazard information for emergency managers in local communities.

More recent studies (Witter and others, 2011) have inferred: (1) higher variability in both the amount of slip and slip distribution from the paleotsunami record and (2) the L1 scenario on the CSZ is a more conservative choice, that is, it is less likely to be exceeded. The L1 source model produces a greater amount of slip 88.6 ft (27 m) compared to the 1A scenario (62 ft, 19 m). It also partitions all slip onto a splay fault that intersects the seafloor at a higher angle than the 1A model, which places all slip on the subduction interface. The L1 scenario is estimated to equal or exceed 95 percent of all previously inferred tsunami

Figure 1. Location map of the Anacortes–Bellingham study area, Cascadia subduction zone, major offshore channels, and major crustal faults known to produce tsunamis, discussed in the text.

Table 1. Published tsunami hazard maps for Washington. CSZ, Cascadia subduction zone. *1A with asperity model incorporates localized area of offshore uplift.

Location	Reference	Modeled Scenario
Southwest Washington	Eungard and others (2018)	CSZ L1
San Juan Islands	Walsh and others (2016)	CSZ L1
Everett	Walsh and others (2014)	Seattle Fault
Tacoma	Walsh and others (2009)	Tacoma and Seattle faults
Anacortes–Whidbey Island	Walsh and others (2005)	CSZ 1A and 1A with asperity*
Bellingham	Walsh and others (2004)	CSZ 1A and 1A with asperity*
Neah Bay	Walsh and others (2003a)	CSZ 1A and 1A with asperity*
Quileute area	Walsh and others (2003b)	CSZ 1A and 1A with asperity*
Seattle	Walsh and others (2003c)	Seattle Fault
Port Angeles	Walsh and others (2002a)	CSZ 1A and 1A with asperity*
Port Townsend	Walsh and others (2002b)	CSZ 1A and 1A with asperity*
southern Washington coast	Walsh and others (2000)	CSZ 1A and 1A with asperity*

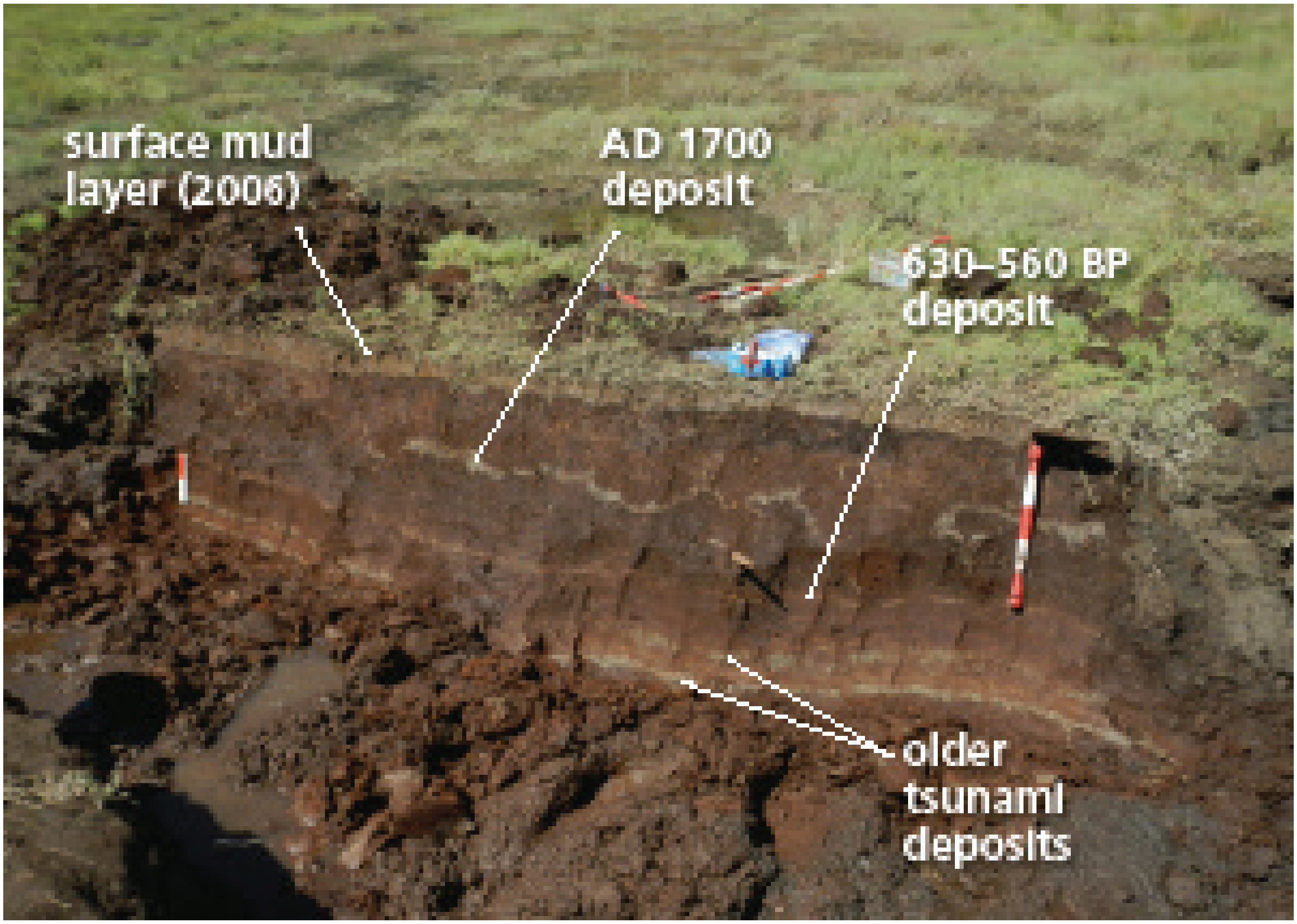

Figure 2. Photo of tsunami deposits (sand layers bounded by silty clays) at Discovery Bay, WA. Four tsunami deposits visible in photo include inferred AD 1700 sand layer that was later disturbed by marsh restoration projects, a sand layer dated at 630 to 560 radiocarbon years BP (Garrison-Laney and Miller, 2017), and two older sand layers beneath. The topmost mud layer was deposited in 2006, following marsh restoration. Photo by Carrie Garrison-Laney (Washington Sea Grant).

inundation events produced by a CSZ sourced tsunami (Witter and others, 2011).

The modeled scenario (L1) earthquake is a close approximation to design requirements for critical facilities in the Washington State building code for seismic hazards. The scenario represents the maximum considered event that a facility may be subjected to during its operational lifetime and serves as a conservative choice for local evacuation planning for tsunami hazards. (See *Earthquake Magnitudes and Slip Distributions* for more information on model scenarios.) The newer L1 study area does not extend as far to the north or south as the previous 1A modeling areas, but it does cover a gap left between the prior model areas. It also incorporates higher quality elevation data from lidar and multibeam bathymetry where available.

CASCADIA SUBDUCTION ZONE

Research over the last few decades on great earthquakes and resulting tsunamis off the British Columbia, Washington, Oregon, and northern California coastlines (Atwater, 1992; Atwater and others, 1995) has led to concern that locally generated tsunamis will leave little time for response. Numerous workers found geologic evidence of tsunami deposits attributed to the CSZ in at least 59 localities from northern California to southern Vancouver Island (Peters and others, 2003). While most of these locations are on the outer coast, inferred CSZ tsunami deposits were identified along the Strait of Juan de Fuca at Salt Creek (Hutchinson and others, 2013), as far east as Discovery Bay (near Port Townsend)(Fig. 2; Williams and others, 2005), on the west shore of Whidbey Island (Fig. 1; Williams and Hutchison, 2000), and as far south as Lynch Cove at the terminus of Hood Canal (Garrison-Laney, 2017). Heaton and Snavely (1985) reported that Makah stories may record a tsunami washing through Waatch Prairie near Cape Flattery (Fig. 1). Ludwin (2002) has found additional stories from native peoples up and down the coast that appear to corroborate this and include apparent references to associated strong ground shaking.

Additionally, high-resolution dendrochronology (Jacoby and others, 1997; Yamaguchi and others, 1997) indicates that the timing of the last CSZ earthquake correlates with historical records of a distant-source tsunami in Japan (Satake and others, 1996) on January 26, AD 1700.

Recurrence Intervals

Estimates of the frequency of CSZ earthquakes are derived from several lines of evidence: coastal submergence events, paleotsunami deposits (Fig. 2), and offshore turbidite deposits. Great subduction zone earthquakes commonly cause coseismic subsidence (Plafker, 1969; Plafker and Savage, 1970). Where this subsidence occurs in coastal marshes, marsh deposits may be abruptly overlain by estuarine mud, indicating sudden submergence and drowning of upland surfaces (Atwater, 1992). Atwater and Hemphill-Haley (1997) reported six sudden submergence events in Willapa Bay over the last 3,500 years (Table 2). Their data imply an average recurrence interval of about 500 to 540 years, but individual intervals vary between 100 and 1,300 years.

Researchers working in Oregon have found a somewhat different record farther south. Using marsh stratigraphy and inferred tsunami deposits, Kelsey and others (2002) found a 5,500-year record of 11 earthquake events at Sixes River in southern Oregon (Fig. 3). These records included an abrupt subsidence event not observed on the southern Washington coast. Kelsey and others (2005) examined Bradley Lake on the southern Oregon coast near Bandon and found that it recorded inferred tsunami deposits with an average recurrence interval of 390 years. This discrepancy implies that some tsunamis generated by earthquakes on the CSZ did not produce abrupt subsidence in southern Washington. A possible explanation is that the earthquake did not rupture the entire length of the subduction zone, resulting in a spatially heterogeneous response in the geologic record. Nelson and others (2006) examined the degree of overlap and amount of abrupt subsidence at eight sites along the Oregon and Washington coasts and concluded that rupture lengths (and therefore earthquake magnitudes) varied—ruptures along the northern CSZ are generally long, whereas ruptures along the southern CSZ are more variable in both length and recurrence interval.

Another approach to inferring recurrence intervals is the correlation of turbidites—deposits of sediment gravity flows or turbidity currents—at the base of the continental shelf. Adams (1990) inferred that turbidite deposits in Cascadia Channel and Astoria Canyon (Fig. 4) were triggered by great earthquakes. If turbidity currents are triggered independently, at different times, and at multiple submarine canyon heads that merge with a main channel, then their deposits should be additive in the main channel. For example, if a channel has three tributaries, each of which has ten independent turbidites, there would be 30 turbidites in the main channel. However, if the turbidites are triggered simultaneously—which would likely be the case if they were initiated by a great earthquake—they should coalesce. In this case, the maximum number of turbidites in the main channel would be no more than the maximum number found in any individual channel. Oregon State University researchers logged 13 turbidites in both Cascadia Channel and Astoria Canyon, from multiple deep-sea cores that were stratigraphically above the Mazama ash (radiocarbon dated at about 6,845 radiocarbon years BP [calibrated to about 7,700 cal yr BP])(Adams, 1990). These findings suggest that 13 CSZ ruptures have occurred since the Mazama ash was deposited. Adams (1990) therefore inferred an average recurrence interval of 590 ±170 years.

Goldfinger and others (2012) tested Adams' (1990) hypothesis by collecting numerous additional cores in the sea floor along the Cascadia continental margin. Their effort greatly expands the geographic and chronologic range of observation, and increases observation density. Goldfinger and others (2012) inferred from their record of turbidite deposits that the CSZ is segmented, with full-length ruptures having a recurrence

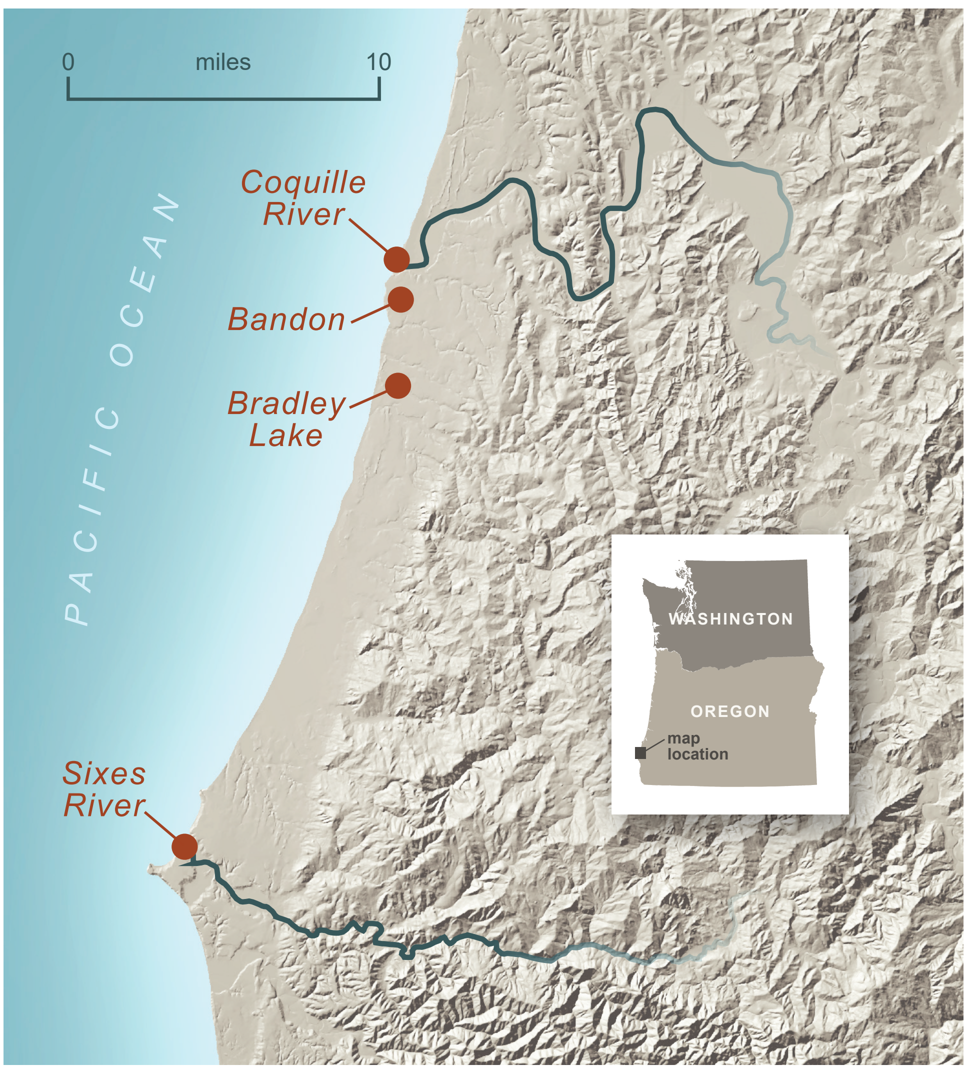

Figure 3. Map of southwest Oregon showing tsunami deposits and abrupt subsidence locations used by Kelsey and others (2002, 2005) to determine CSZ earthquake recurrence intervals.

Table 2. Estimates of earthquake recurrence on the Cascadia subduction zone. - - - indicates no data.

Events over time interval	Average recurrence interval in years; range if given	Section of CSZ	References	Major evidence
6 submergence events in 3,500 years	500–540 average, 100–300 to 1,300	northern	Atwater and Hemphill-Haley (1997)	submergence events
11 submergence events in 5,500 years	510	southern	Kelsey and others (2002)	marsh stratigraphy and tsunami deposits
13 tsunamis, 17 disturbances in 7,000 years	- - -	southern	Kelsey and others (2005)	marine incursions and disturbance events in Bradley Lake
- - -	variable	whole	Nelson and others (2006)	multiple
- - -	590 ±170	northern	Adams (1990)	turbidites in Astoria Canyon and Cascadia Channel
19 or 20 full-margin turbidites in 10,000 years; 22 turbidites restricted to the south	500–530 average for full-margin rupture; ~240 full-margin plus southern only	whole and partial	Goldfinger and others (2012)	turbidites along Cascadia margin
20 full-margin turbidites in 10,000 years; 3 turbidites on a segment running from northern California to Juan de Fuca Channel; 1 turbidite off Washington and B.C. only	500–530 average for full-margin rupture; ~434 full-margin plus shorter ruptures adjacent to Washington	whole and partial	Goldfinger and others (2017)	turbidites along Cascadia margin

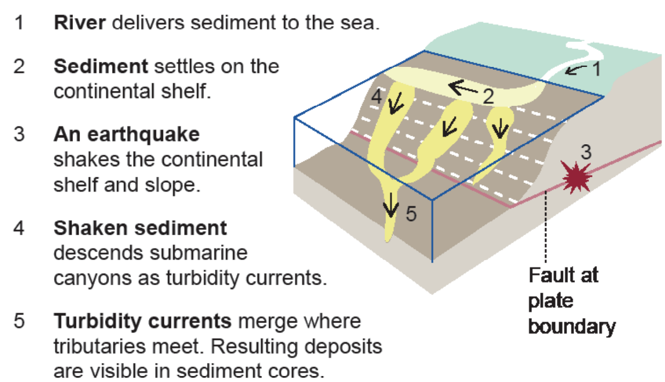

Figure 4. Schematic view of the confluence test for extensive seismic shaking, first used as a guide to fault rupture length by Adams (1990). Adams assumed that extensive shaking enables turbidity currents to descend different submarine channels at the same time and merge below channel confluences. Atwater and others (2014) dispute the reliability of this indicator.

interval similar to those estimated by Adams (1990) and Atwater and Hemphill-Haley (1997), but with additional partial-length ruptures offshore Oregon and northern California.

Combining full-length and partial ruptures on the CSZ, Goldfinger and others (2012) estimated a recurrence interval of ~240 years for earthquakes off Oregon and northern California, but still 500 to 530 years offshore Washington and British Columbia. Earthquakes that rupture only the northern part of the CSZ are also a possibility. Goldfinger and others (2017) revised this chronology slightly, extending several ruptures farther north to include Washington and inferring an additional event offshore Washington and southern British Columbia only. In Discovery Bay and in the northeast of the Olympic Peninsula, Williams and others (2005) observed nine muddy sand beds bearing marine diatoms that interrupt a 2,500-year-old sequence of peat deposits beneath a tidal marsh. If all of these are tsunami deposits, then it is likely that some of them record events that are either not full-length ruptures of the CSZ or come from some other source. The ages of four of these beds, refined by Garrison-Laney and Miller (2017), overlap with known late-Holocene tsunamis generated by full-length ruptures of the CSZ. Diatom assemblages in peat deposits bracketing these four beds do not indicate a concurrent change in elevation at Discovery Bay. This suggests that coseismic subsidence has been negligible as far east as Discovery Bay and is not expected any farther east. However, one inferred tsunami deposit is accompanied by several decimeters of abrupt subsidence, which is interpreted as the result of deformation associated with an upper plate fault (Williams and others, 2002). Other sand sheets in the sequence may represent tsunamis generated by partial ruptures of the CSZ, by upper plate fault earthquakes or by landslides (Garrison-Laney and Miller, 2017), none of which triggered turbidity currents. This implies that either some CSZ earthquakes do not leave turbidite deposits in Cascadia Channel, or that some tsunami deposits were generated by other events, such as local earthquakes or landslides. Atwater and others (2014) also questioned whether the absence of turbidites along the northern CSZ necessarily proves the absence of ground shaking, or rather is influenced by differences in sediment supply and in flow paths down tributary channels. They also questioned some of the correlations among widely spaced sites—used to infer the length of fault rupture—that were used by Goldfinger and others (2012).

Earthquake Magnitudes and Slip Distributions

AD 1700 EARTHQUAKE

It is believed that the last earthquake on the Cascadia subduction zone was about magnitude (Mw) 9.0 (Satake and others, 1996, 2003). Satake and others (2003) tested various rupture lengths, slip amounts, and observed tsunami wave heights in Japan for the AD 1700 event. They estimated that this event had a rupture length of 684 mi (~1,100 km) and 62 ft (19 m) of coseismic slip on an offshore, full-slip zone with linearly decreasing slip on a down-dip partial-slip zone, suggesting

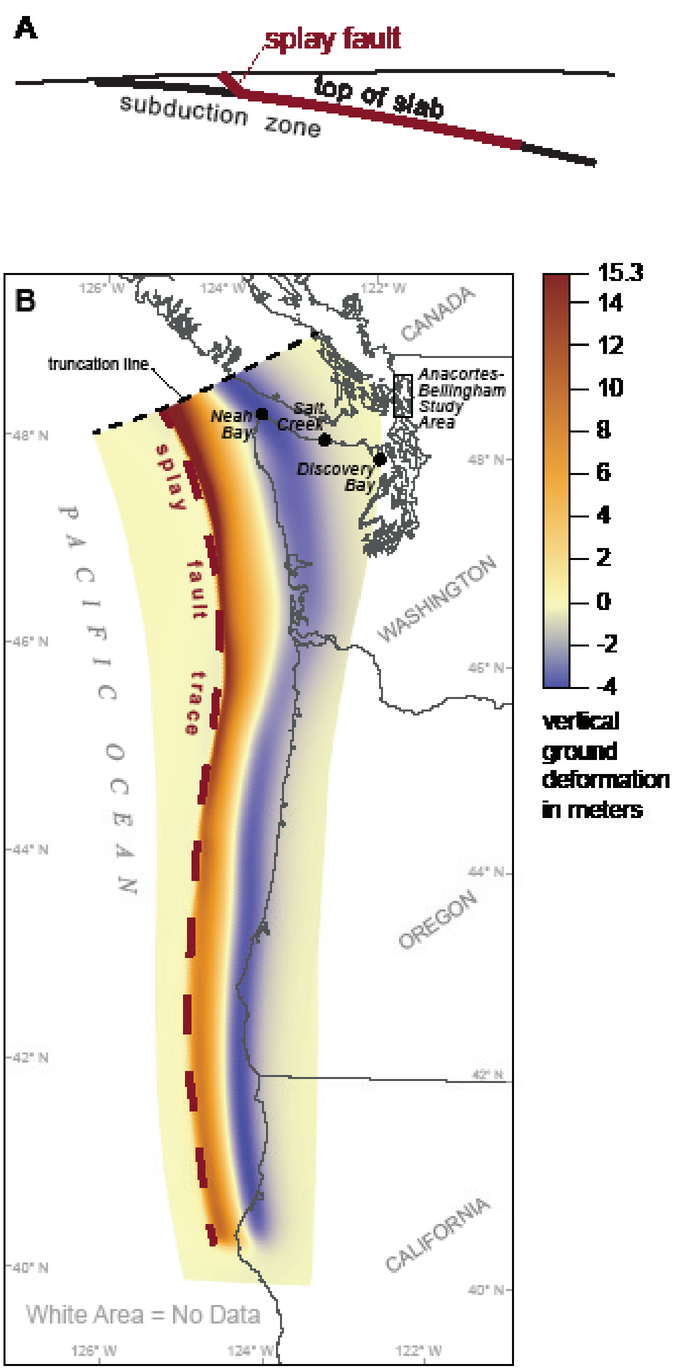

Figure 5. L1 splay fault model diagram (A) and map of vertical ground deformation (B) during a great Cascadia earthquake in the L1 scenario of Witter and others (2011). The northern part of the scenario is truncated south of where the Juan de Fuca plate is broken up into microplates.

a magnitude of 8.7 to 9.2. They inferred that the most likely magnitude was 9.0 based on the correlation between estimates of coseismic subsidence from paleoseismic studies and the subsidence predicted by their scenario dislocation models.

PRE-AD 1700 EARTHQUAKES

Partial-Length Rupture Models

The magnitudes and slip distributions of earlier CSZ earthquakes are less well constrained. Inferences of shorter ruptures that affect only the southern part of the CSZ generally imply smaller magnitude earthquakes. Tsunamis from several postulated shorter ruptures limited to the southern part of the CSZ were modeled by Priest and others (2014), who concluded that the tsunamis they generated were significantly smaller in Washington than those generated by full-length ruptures. A partial CSZ rupture restricted to the north was suggested by Goldfinger and others (2013) and Peterson and others (2013). This northern rupture was later confirmed by Goldfinger and others (2017), but paleoseismic data for it is insufficient to generate a tsunami model. These smaller events are not considered further here.

Full-Length Rupture Models

Witter and others (2012) combined: (1) turbidite data from Goldfinger and others (2012); (2) correlation of inferred tsunami deposits with turbidites in Bradley Lake; and (3) inferred tsunami deposits in the Coquille River estuary at Bandon, Oregon, that extend as much as 6.2 mi (10 km) farther inland than the AD 1700 tsunami deposits (Witter and others, 2003). They inferred from this that tsunamis generated by Cascadia over the last 10,000 years have been highly variable, with some larger than the one in AD 1700. They constructed 15 scenarios of full-length ruptures, that defined the vertical seafloor deformation used to simulate tsunami inundation at Bandon, Oregon. Rupture models included slip partitioned to a splay fault in the accretionary wedge and models that vary the up-dip limit of slip on a buried megathrust fault. Slip estimates were made from several sources. Total turbidite volume was estimated from the thickness averaged over all the paleoseismic records, which Goldfinger and others (2012) correlated to earthquake magnitude. This was combined with estimates of the convergence rate for different segments of the subduction zone multiplied by the time since the previous event to estimate total accumulated strain since the previous event (Witter and others, 2012). Witter and others (2011, 2012) performed numerical tsunami simulations at Bradley Lake and Bandon, Oregon, and then compared them using a logic tree that ranked model consistency with geophysical and geological data from the distribution of inferred tsunami deposits. They found that the deposits were broadly compatible with their larger scenarios.

Witter and others (2011) concluded that scenario L1—a splay fault model with a maximum slip of 88.6 ft (27 m) and an average slip of 42.6 ft (13 m)—produced a tsunami that equaled or exceeded 95 percent of the variability in their simulations (Fig. 5). Other 'L' earthquake scenarios (L2 and L3) have the same amount of slip but somewhat different distributions across the strike of the subduction zone. In other words, the L1 scenario produces tsunamis as big as or bigger than most other models. Witter and others (2011) also estimated the size of the earthquakes that generated turbidites along the full length of the CSZ. They concluded that three earthquakes in the last ~10,000 years were probably similar to scenario L and only one was larger (table 1 in Witter and others, 2011). The inter-event times between pairs of inferred L earthquakes are ~1,800 and ~4,600 years. Another way to estimate recurrence frequency is that if three earthquakes in the last 10,000 years are of size L, then these types of events have an average recurrence interval between 2,500 and 5,000 years. If this truly represents 95 percent of the hazard

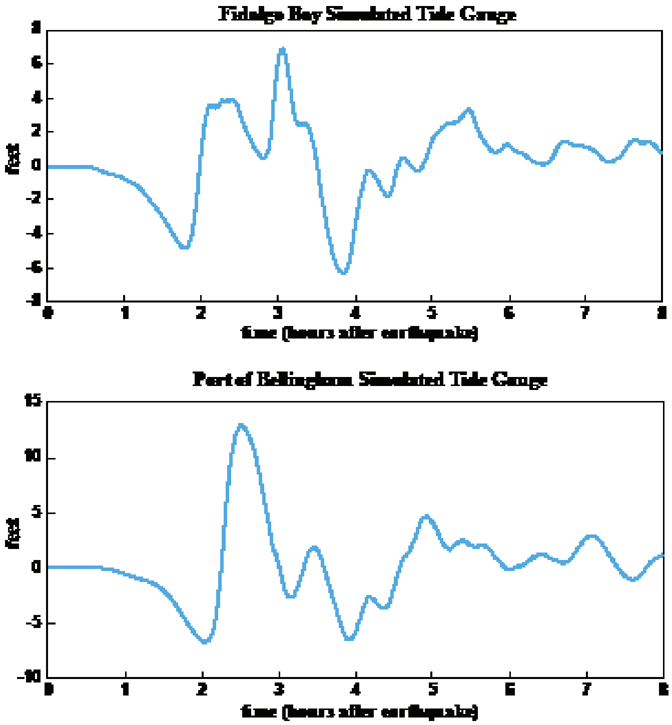

Figure 6. Modeled tsunami wave amplitude variations over time for offshore areas near Fidalgo Bay and Port of Bellingham (see Map Sheets 1 and 2 for locations).

over a 10,000-year period, then scenario L earthquakes have a long recurrence interval and likely are of a similar probability of occurrence as the International Building Code seismic standard of 2 percent probability of exceedance in 50 years. Colloquially, this scenario is known as a ~2,500-year event.

MODELING APPROACH AND RESULTS

This tsunami inundation model is based on a numerical model of waves generated by a L1 CSZ scenario earthquake as described in Witter and others (2011) and as adapted in Walsh and others (2016). The simulation uses the finite difference model of Titov and Synolakis (1998), known as the Method of Splitting Tsunami (MOST) model (Titov and González, 1997). The model uses a grid of topographic and bathymetric elevations and calculates a wave elevation and velocity for each cell at specified time intervals to simulate the generation, propagation, and inundation of a tsunami following an L1-style CSZ earthquake. The model is calculated for mean high water and does not include tidal effects. The modeling for this map was done by the NOAA Center for Tsunami Research at NOAA's Pacific Marine Environmental Laboratory in Seattle.

The selected scenario is a splay-fault model in which all slip is partitioned into a thrust fault in the accretionary wedge that has an approximate 30º landward dip and the same sense of movement as the megathrust; this results in a much higher, narrower area of uplift than a fault rupture on the megathrust, which dips landward much more shallowly and reaches farther seaward than the splay fault. Coseismic subsidence of the land surface is not expected in the Anacortes and Bellingham area, as it is too distant from the subduction zone.

Inundation

Inundation depth bins on Map Sheets 1 and 2 were selected based on their implications for life safety. These bins are defined as: (1) less than knee high (0–2.5 ft, <0.75 m); (2) knee to head high (2.5–6 ft, 0.75–1.8 m); and (3) above head height (>6 ft, >1.8 m). These depths approximate the hazard posed to a person if caught within the tsunami zone. At 0 to 2.5 ft inundation, survival is likely if steps are taken to avoid the direct force of a wave, such as entering a building, or standing on the leeward side of an obstacle (tree or power pole). From 2.5 to 6 ft inundation, survival is unlikely if caught in the open; however, climbing onto the roof of a single-story structure or entering a structure with more than one story may improve survivability. At >6 ft inundation, survival is highly unlikely if caught either out in the open or within or on most conventional structures. Survival remains highly likely within or on a reinforced and specially designed building, such as a vertical evacuation structure. Modeled inundation is also shown using the full range of values on Map Sheets 5 and 6.

Tsunami inundation from this scenario is expected to be locally extensive, covering most of the low-lying river valleys in both Whatcom and Skagit counties. Elsewhere, coastal inundation is generally limited by high bluffs. Inundation depths may reach 18 ft (5.5 m) in some low-lying coastal areas, with significant inundation modeled on the Lummi Reservation, along Padilla and Samish bays, and in other waterfront developments. Inundation would be expected to continue well beyond the study area boundaries at both the Lummi Reservation to the north and south of SR-20 near Whitney—see previous modeling by Walsh and others (2005, 2004).

Current Speed

The modeled current speed (Map Sheets 3 and 4) is shown in four ranges: 0–3 knots, 3–6 knots, 6–9 knots, and >9 knots, following the port damage categorization of Lynett and others (2014). These ranges approximate hazards to ships and docking facilities, representing no expected damage, minor/moderate damage possible, major damage possible, and extreme damage possible, respectively. Modeled current speed locally exceeds 20 knots in the study area and is strongest in narrower waterway channels and nearshore where the tsunami–tide interactions are likely to be most significant. Key areas of strong currents are Guemes Channel, Burrows Pass, off Clark Point, and off Eliza Rock.

Timing of Tsunami and Initial Water Disturbance

Wave arrival times are estimated from the moment the earthquake begins to the moment the water first rises above high tide (mean high water). For the arrival times shown on Map Sheets 5 and 6, this is not the timing of maximum inundation. Several minutes may transpire between first wave arrival and maximum inundation. Strong earthquake shaking may persist for as many as five minutes in this scenario, reducing the available time to evacuate to less than the indicated wave arrival times. Figure 6 shows simulated tide gauge records at the entrance to Fidalgo Bay and the Port of Bellingham. The initial water disturbance at these locations is a gradual ~5 to 6.5 ft (1.5–2 m) fall in sea level from 1 hour to 1 hour 45 minutes at Fidalgo Bay and 1 to 2 hours at the Port of Bellingham from a leading wave trough following the earthquake. This is followed by a rapidly rising wave arriving at 2 hours 9 minutes and 2 hours 30 minutes respectively after the earthquake. At Fidalgo Bay, the second wave will be the largest, arriving at 3 hours after the earthquake. Figure 7, a conceptual visualization, demonstrates this chain of events.

The highest wave is expected to be 6.9 ft (2.1 m) high at the entrance to Fidalgo Bay (second wave) and 13.1 ft (4 m) high at the Port of Bellingham. Waves of <5 ft (1.5 m) are expected for at least 8 hours following the earthquake (Fig. 6). Minor inundation and strong currents may continue for at least 24 hours after the earthquake. These currents may pose a hazard to maritime operations. For comparison, the January 26, AD 1700 earthquake along the CSZ produced a tsunami that may have lasted as long as 20 hours in Japan (Satake and others, 2003; Atwater and others, 2005). The March 27, 1964, magnitude 9.2 earthquake near Anchorage, Alaska, produced a tsunami in Washington that lasted for at least 12 hours (Walsh and others, 2000).

LIMITATIONS OF THE MODEL

Because the characteristics of the tsunami depend on the initial seafloor deformation of the earthquake, which is poorly understood, the largest source of uncertainty is the input earthquake. The earthquake scenario used in this model was selected to approximate the 2 percent probability of exceedance in 50 years (~2,500-year event), but the next earthquake may have a more complex slip distribution than the simplified scenario we used and thus the ensuing tsunami may differ. Witter and others (2011) suggest that the most likely full-length CSZ earthquake will have an average slip of about two-thirds of the L1 scenario and therefore generate a smaller tsunami than modeled here.

These model results do not include potential tsunamis from coseismic landslides or ruptures on nearby crustal faults. This modeling does not incorporate localized topographic changes caused by liquefaction, such as settlement or sand-blows. Liquefaction is a site-specific issue and is inappropriate at this map scale. The model does not include the influences of changes in tides and is referred to mean high water. The tide stage can amplify or reduce the impact of a tsunami on a specific community. For example, the diurnal range (the difference in height between mean higher high water and mean lower low water) is 3.04 ft (0.92 m) at the Cherry Point tide gauge (https://tidesandcurrents.noaa.gov/datums.html?id=9449424). The model also does not include interaction with tidal currents, which can be additive, or if in opposite directions, can steepen the tsunami wave front and cause a breaking wave.

The resolution of the modeling is also limited by the bathymetric and topographic data used to make the elevation grid. The elevation grid was created with a variety of data sources, with cell sizes ranging from 3 to 33 ft (1–10 m) for the topographic grid and 16 to 3,937 ft (5–1,200 m) for the bathymetric grid. Coarse grids do not capture small topographic features that can influence the tsunami locally. This generally leads to greater modeled inundation than would be produced by finer grids, except in narrow or constricted channels or along steep topographic features.

Small, isolated gaps in modeled inundation exist (for example, berms along SR 20 near Padilla Bay). Additionally, transient features (log piles, temporary aggregate piles, etc.), misclassified buildings or treetops, and some actual high areas

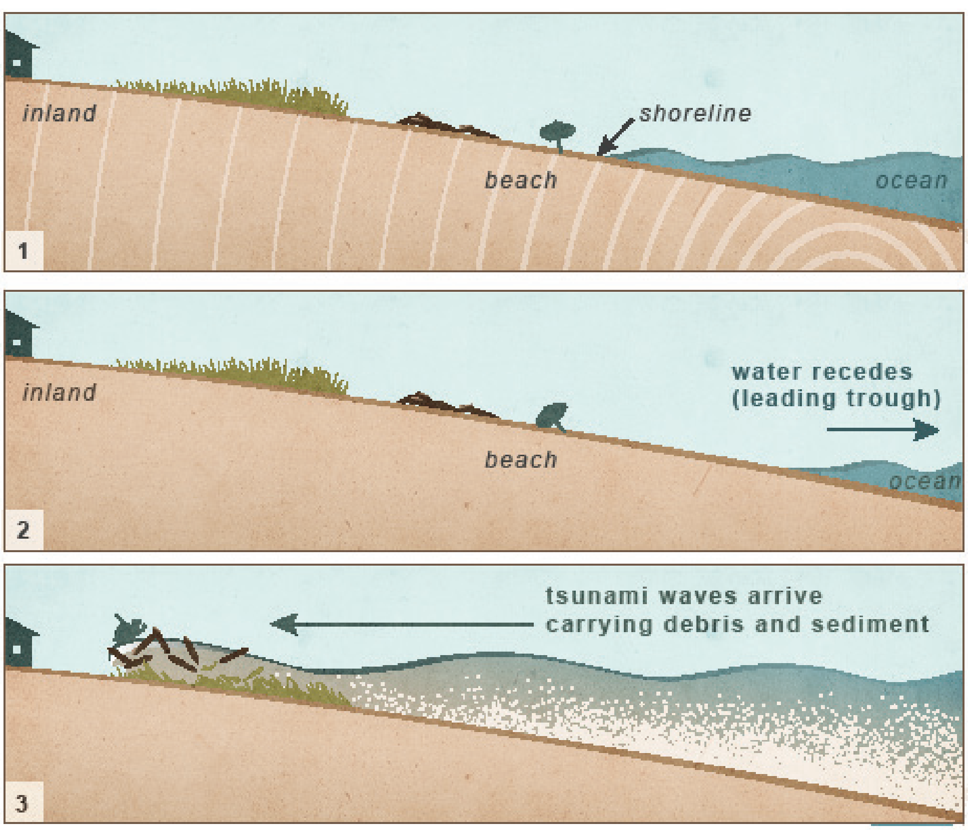

Figure 7. Schematic diagram of chronologic events following a CSZ earthquake and tsunami: (1) Earthquake on the CSZ produces strong shaking that will last several minutes; (2) The first indication of an incoming tsunami wave to the Anacortes and Bellingham region will be a gradual drop in water level immediately prior to arrival of the first tsunami wave; and (3) Tsunami waves begin to arrive ~2 hours following the earthquake—these powerful waves carry sediment and debris onshore and to higher elevations. The wave attack continues for at least 8 hours, locally posing a hazard to search, rescue, and recovery efforts.

may not survive the impact of tsunami waves. The maps retain these gaps in inundation to remain true to the model results. However, it is highly likely that these small areas will be inundated during a tsunami.

While the modeling can be a useful tool to guide evacuation planning, model uncertainties and insufficient spatial resolution make this modeling unsuitable for site-specific tsunami mitigation planning.

ACKNOWLEDGMENTS

This project was supported by the National Tsunami Hazards Mitigation Program (NTHMP) in cooperation with Whatcom, Skagit, and Island counties, and the Washington Emergency Management Division.

REFERENCES

Adams, John, 1990, Paleoseismicity of the Cascadia subduction zone—Evidence from turbidites off the Oregon–Washington margin: Tectonics, v. 9, no. 4, p. 569-583.

Atwater, B. F., 1987, Evidence for great Holocene earthquakes along the outer coast of Washington State: Science, v. 236, no. 4804, p. 942-944.

Atwater, B. F., 1992, Geologic evidence for earthquakes during the past 2,000 years along the Copalis River, southern coastal Washington: Journal of Geophysical Research, v. 97, no. B2, p. 1901-1919.

Atwater, B. F.; Carson, R. C.; Griggs, G. B.; Johnson, H. P.; Salmi, M. S., 2014, Rethinking turbidite paleoseismology along the Cascadia subduction zone: Geology, v. 42, no. 9, p. 827-830.

Atwater, B. F.; Hemphill-Haley, Eileen, 1997, Recurrence intervals for great earthquakes of the past 3,500 years at northeastern Willapa Bay, Washington: U.S. Geological Survey Professional Paper 1576, 108 p. [https://pubs.er.usgs.gov/publication/pp1576]

Atwater, B. F.; Nelson, A. R.; Clague, J. J.; Carver, G. A.; Yamaguchi, D. K.; Bobrowsky, P. T.; Bourgeois, Joanne; Darienzo, M. E.; Grant, W. C.; Hemphill-Haley, Eileen; Kelsey, H. M.; Jacoby, G. C.; Nishenko, S. P.; Palmer, S. P.; Peterson, C. D.; Reinhart, M. A., 1995, Summary of coastal geologic evidence for past great earthquakes at the Cascadia subduction zone: Earthquake Spectra, v. 11, no. 1, p. 1-18.

Atwater, B. F.; Musumi-Rokkaku, Satoko; Satake, Kenji; Tsuji, Yoshinobu; Ueda, Kazue; Yamaguchi, D. K., 2005, The orphan tsunami of 1700—Japanese clues to a parent earthquake in North America: University of Washington Press and U.S. Geological Survey Professional Paper 1707, 133 p. [https://pubs.usgs.gov/pp/pp1707/pp1707_front.pdf]

Eungard, D. W.; Forson, Corina; Walsh, T. J.; Gica, Edison; Arcas, Diego, 2018, Tsunami hazard maps of southwest Washington—Model results from a ~2,500-year Cascadia subduction zone earthquake scenario: Washington Geological Survey Map Series 2018-01, originally published March 2018, 6 sheets, scale 1:48,000, 11 p. text. [http://www.dnr.wa.gov/publications/ger_ms2018-01_tsunami_hazard_southwest_washington.zip]

Garrison-Laney, C. E., 2017, Tsunamis and sea levels of the past millennium in Puget Sound, Washington: University of Washington Doctor of Philosophy thesis, 166 p.

Garrison-Laney, C. E.; Miller, I., 2017, Tsunamis in the Salish Sea: Recurrence, sources, hazards. *In* Haugerud, R. A.; Kelsey, H. M., 2017, From the Puget Lowland to east of the Cascade Range—Geologic excursions in the Pacific Northwest: Geological Society of America Field Trip Guide v. 49, p. 67-78.

Goldfinger, Chris; Nelson, C. H.; Morey, A. E.; Johnson, J. E.; Patton, J. R.; Karabanov, Eugene; Gutierrez-Pastor, Julia; Eriksson, A. T.; Gracia, Eulalia; Dunhill, Gita; Enkin, R. J.; Dallimore, Audrey; Vallier, Tracy, 2012, Turbidite event history—Methods and implications for Holocene paleoseismicity of the Cascadia subduction zone: U.S. Geological Survey Professional Paper 1661-F, 170 p., 64 figures. [https://pubs.usgs.gov/pp/pp1661f/]

Goldfinger, Chris; Galer, Steve; Beeson, Jeffrey; Hamilton, Tark; Black, Bran; Romsos, Chris; Patton, Jason; Nelson, C. H.; Hausmann, Rachel; Morey, Ann, 2017, The importance of site selection, sediment supply, and hydrodynamics—A case study of submarine paleoseismology on the northern Cascadia margin, Washington, USA: Marine Geology, v. 384.

Goldfinger, Chris; Morey, A. E.; Black, Bran; Beeson, Jeffrey; Nelson, C. H.; Patton, Jason, 2013, Spatially limited mud turbidites on the Cascadia margin: segmented earthquake ruptures?: Natural Hazards and Earth System Sciences, v. 13, no. 8, p. 2109-2146.

Heaton, T. H.; Snavely, P. D., Jr., 1985, Possible tsunami along the northwestern coast of the United States inferred from Indian traditions: Seismological Society of America Bulletin, v. 75, no. 5, p. 1455-1460.

Hutchinson, Ian; Peterson, C. D.; Sterling, S. L., 2013, Late Holocene tsunami deposits at Salt Creek, Washington, USA: Science of Tsunami Hazards, v. 32, p. 221-235.

Jacoby, G. C.; Bunker, D. E.; Benson, B. E., 1997, Tree-ring evidence for an A.D. 1700 Cascadia earthquake in Washington and northern Oregon: Geology, v. 25, no. 11, p. 999-1002.

Kelsey, H. M.; Nelson, A. R.; Hemphill-Haley, Eileen; Witter, R. C., 2005, Tsunami history of an Oregon coastal lake reveals a 4,600 yr record of great earthquakes on the Cascadia subduction zone: Geological Society of America, v. 117, no. 7-8, p. 1009-1032.

Kelsey, H. M.; Witter, R. C.; Hemphill-Haley, Eileen, 2002, Plate boundary earthquakes and tsunamis of the past 5,500 yr, Sixes River estuary, southern Oregon: Geological Society of America Bulletin, v. 114, no. 3, p. 298-314.

Ludwin, R. S., 2002, Cascadia megathrust earthquakes in Pacific Northwest Indian myths and legends: TsuInfo Alert, v. 4, no. 2, p. 6-10. [https://www.dnr.wa.gov/publications/ger_tsuinfo_2002_v4_no2.pdf]

Lynett, P. J.; Borrero, Jose; Son, Sangyoung; Wilson, Rick; Miller, Kevin, 2014, Assessment of the tsunami-induced current hazard, Geophysical Research Letters, v. 41, iss. 6, p. 2048-2055.

Myers, E. P., III; Baptista, A. M.; Priest, G. R., 1999, Finite element modeling of potential Cascadia subduction zone tsunamis: Science of Tsunami Hazards, v. 17, no. 1, p. 3-18.

Nelson, A. R.; Kelsey, H. M.; Witter, R. C., 2006, Great earthquakes of variable magnitude at the Cascadia subduction zone: Quaternary Research, v. 65, no. 3, p. 354-365.

Peters, Robert; Jaffe, B. E.; Gelfenbaum, Guy; Peterson, C. D., 2003, Cascadia tsunami deposit database: U.S. Geological Survey Open-File Report 03-13, 25 p. [accessed May 6, 2004, at http://geopubs.wr.usgs.gov/open-file/of03-13/]

Peterson, C. D.; Cruikshank, K. M. ; Darienzo, M. E. ; Wessen, G. C.; Butler, V. L.; Sterling, S. L., 2013, Coseismic subsidence and paleotsunami run-up records from latest Holocene deposits in the Waatch Valley, Neah Bay, northwest Washington, U.S.A.—Links to great earthquakes in the northern Cascadia margin: Journal of Coastal Research, v. 29, no. 1, p. 157-172.

Plafker, George, 1969, Tectonics of the March 27, 1964, Alaska earthquake: U.S. Geological Survey Professional Paper 543-1, 74 p., 2 sheets, scales 1:2,000,000 and 1:500,000. [https://pubs.usgs.gov/pp/0543i/].

Plafker, George; Savage, J. C., 1970, Mechanism of the Chilean earthquakes of May 21 and 22, 1960: Geological Society of America Bulletin, v. 81, no. 4, p. 1001-1030.

Priest, G. R.; Myers, E. P., III; Baptista, A. M.; Fleuck, Paul; Wang, Kelin; Kamphaus, R. A.; Peterson, C. D., 1997, Cascadia subduction zone tsunamis—Hazard mapping at Yaquina Bay, Oregon: Oregon Department of Geology and Mineral Industries Open-File Report O-97-34, 144 p. [http://www.oregongeology.org/pubs/ofr/O-97-34.pdf]

Priest, G. R.; Zhang, Yinglong; Witter, R. C.; Wang, Kelin; Goldfinger, Chris; Stimely, Laura, 2014, Tsunami impact to Washington and northern Oregon from segment ruptures on the southern Cascadia subduction zone: Natural Hazards, v. 72, no. 2, p. 849-870.

Satake, Kenji; Shimazaki, Kunihiko; Tsuji, Yoshinobu; Ueda, Kazue, 1996, Time and size of a giant earthquake in Cascadia inferred from Japanese tsunami records of January 1700: Nature, v. 379, no. 6562, p. 246-249.

Satake, Kenji; Wang, Kelin; Atwater, B. F., 2003, Fault slip and seismic moment of the 1700 Cascadia earthquake inferred from Japanese tsunami description: Journal of Geophysical Research, v. 108, no. B11, 2535, 17 p.

Titov, V. V.; González, F. I., 1997, Implementation and testing of the Method of Splitting Tsunami (MOST) model: NOAA Technical Memorandum ERL PMEL-112 (PB98-122773), 11 p.

Titov, V. V.; Synolakis, C. E., 1998, Numerical modeling of tidal wave runup: Journal of Waterway, Port, Coastal and Ocean Engineering, v. 124, no. 4, p. 157-171.

Walsh, T. J.; Arcas, Diego; Titov, V. V.; Chamberlin, C. C., 2014, Tsunami hazard map of Everett, Washington: Model results for magnitude 7.3 and 6.7 Seattle fault earthquakes: Washington Division of Geology and Earth Resources Open File Report 2014-03, 1 plate, scale 1:32,000. [http://www.dnr.wa.gov/publications/ger_ofr2014- 03_tsunami_hazard_everett.pdf]

Walsh, T. J.; Arcas, Diego; Venturato, A. J.; Titov, V. V.; Mofjeld, H. O.; Chamberlin, C. C.; González, F. I., 2009, Tsunami hazard map of Tacoma, Washington—Model results for Seattle fault and Tacoma fault earthquake tsunamis: Washington Division of Geology and Earth Resources Open File Report 2009-9, 1 sheet, scale 1:24,000. [http://www.dnr.wa.gov/publications/ger_ofr2009-9_tsunami_hazard_tacoma.pdf]

Walsh, T. J.; Caruthers, C. G.; Heinitz, A. C.; Myers, E. P., III; Baptista, A. M.; Erdakos, G. B.; Kamphaus, R. A., 2000, Tsunami hazard map of the southern Washington coast—Modeled tsunami inundation from a Cascadia subduction zone earthquake: Washington Division of Geology and Earth Resources Geologic Map GM-49, 1 sheet, scale 1:100,000, with 12 p. text. [http://www.dnr.wa.gov/publications/ger_gm49_tsunami_hazard_southern_coast.zip]

Walsh, T. J.; Gica, Edison; Arcas, Diego; Titov, V. V.; Eungard, D. W., 2016, Tsunami hazard maps of the San Juan Islands, Washington—Model results from a Cascadia subduction zone earthquake scenario: Washington Division of Geology and Earth Resources Map Series 2016-01, 4 sheets, scale 1:24,000 and 1:48,000, 9 p. text. [http://www.dnr.wa.gov/publications/ger_ms2016-01_tsunami_hazard_san_juan_islands.zip]

Walsh, T. J.; Myers, E. P., III; Baptista, A. M., 2002a, Tsunami inundation map of the Port Angeles, Washington area: Washington Division of Geology and Earth Resources Open File Report 2002-1, 1 sheet, scale 1:24,000. [http://www.dnr.wa.gov/publications/ger_ofr2002-1_tsunami_hazard_portangeles.pdf]

Walsh, T. J.; Myers, E. P., III; Baptista, A. M., 2002b, Tsunami inundation map of the Port Townsend, Washington area: Washington Division of Geology and Earth Resources Open File Report 2002-2, 1 sheet, scale 1:24,000. [http://www.dnr.wa.gov/publications/ger_ofr2002-2_tsunami_hazard_porttownsend.pdf]

Walsh, T. J.; Myers, E. P., III; Baptista, A. M., 2003a, Tsunami inundation map of the Neah Bay, Washington, area: Washington Division of Geology and Earth Resources Open File Report 2003-2, 1 sheet, scale 1:24,000. [http://www.dnr.wa.gov/publications/ger_ofr2003-2_tsunami_hazard_neahbay.pdf]

Walsh, T. J.; Myers, E. P., III; Baptista, A. M., 2003b, Tsunami inundation map of the Quileute, Washington, area: Washington Division of Geology and Earth Resources Open File Report 2003-1, 1 sheet, scale 1:24,000. [http://www.dnr.wa.gov/publications/ger_ofr2003-1_tsunami_hazard_quileute.pdf]

Walsh, T. J.; Titov, V. V.; Venturato, A. J.; Mofjeld, H. O.; González, F. I., 2003c, Tsunami hazard map of the Elliott Bay area, Seattle, Washington—Modeled tsunami inundation from a Seattle Fault earthquake: Washington Division of Geology and Earth Resources Open File Report 2003-14, 1 sheet, scale 1:50,000. [http://www.dnr.wa.gov/publications/ger_ofr2003-14_tsunami_hazard_elliottbay.pdf]

Walsh, T. J.; Titov, V. V.; Venturato, A. J.; Mofjeld, H. O.; González, F. I., 2004, Tsunami hazard map of the Bellingham area, Washington—Modeled tsunami inundation from a Cascadia subduction zone earthquake: Washington Division of Geology and Earth Resources Open File Report 2004-15, 1 sheet, scale 1:50,000. [http://www.dnr.wa.gov/publications/ger_ofr2004-15_tsunami_hazard_bellingham.pdf]

Walsh, T. J.; Titov, V. V.; Venturato, A. J.; Mofjeld, H. O.; González, F. I., 2005, Tsunami hazard map of the Anacortes-Whidbey Island area, Washington—Modeled tsunami inundation from a Cascadia subduction zone earthquake: Washington Division of Geology and Earth Resources Open File Report 2005-1, 1 sheet, scale 1:62,500. [http://www.dnr.wa.gov/publications/ger_ofr2005-1_tsunami_hazard_anacortes_whidbey.pdf]

Williams, H. F. L.; Hutchinson, Ian, 2000, Stratigraphic and microfossil evidence for late Holocene tsunamis at Swantown Marsh, Whidbey Island, Washington: Quaternary Research, v. 54, no. 2, p. 218-227.

Williams, H. F. L.; Hutchinson, Ian; Nelson, A. R., 2005, Multiple sources for late-Holocene tsunamis at Discovery Bay, Washington State, USA: The Holocene, v. 15, no. 1, p. 60-73.

Witter, R. C.; Kelsey, H. M.; Hemphill-Haley, Eileen, 2003, Great Cascadia earthquakes and tsunamis of the past 6,700 years, Coquille River estuary, southern coastal Oregon: Geological Society of America Bulletin, v. 115, no. 10, p. 1289–1306.

Witter, R. C.; Zhang, Yinglong; Wang, Kelin; Goldfinger, Chris; Priest, G. R.; Allan, J. C., 2012, Coseismic slip on the southern Cascadia megathrust implied by tsunami deposits in an Oregon lake and earthquake-triggered marine turbidites: Journal of Geophysical Research, v.117, no. B10303, 17 p.

Witter, R. C.; Zhang, Yinglong; Wang, Kelin; Priest, G. R.; Goldfinger, Chris; Stimely, L. L.; English, J. T.; Ferro, P. A., 2011, Simulating tsunami inundation at Bandon, Coos County, Oregon, using hypothetical Cascadia and Alaska earthquake scenarios: Oregon Department of Geology and Mineral Industries Special Paper 43, 57 p. [http://www.oregongeology.org/pubs/sp/p-SP-43.htm]

Yamaguchi, D. K.; Atwater, B. F.; Bunker, D. E.; Benson, B. E.; Reid, M. S., 1997, Tree-ring dating the 1700 Cascadia earthquake: Nature, v. 389, p. 922-923.